Spring 5-1-2021

An Open-Baffle Motional Feedback Loudspeaker

Matthew Quinlivan

William Harvie

AN OPEN-BAFFLE MOTIONAL FEEDBACK LOUDSPEAKER

By

William Harvie

And

Matthew Quinlivan

A thesis submitted to the faculty of The University of Mississippi in partial fulfillment of the requirements of the Sally McDonnell Barksdale Honors College.

Oxford, MS

April 2021

Approved By

_____

Advisor: Dr. Paul Goggans

_____

Reader: Dr. Elliott Hutchcraft

_____

Reader: Dr. Barry Muldrey

Abstract

A dynamic loudspeaker mounted in an open baffle has the same parameters as a loudspeaker in free space. A subwoofer mounted in an open baffle has a small total quality factor and therefore the frequency above which the driver has a significant output is too high despite the subwoofer's low resonant frequency. To address this issue, we implemented a motional feedback circuit with the goal of introducing both velocity feedback and acceleration feedback into the loudspeaker system and thus altering the resonant frequency and total quality factor of the system. After verifying the efficacy of our feedback circuit with computer simulations, we first tested it using a Sallen-Key highpass filter to model the power amplifier, loudspeaker, and accelerometer and we were able to obtain desired results. We then connected the motional feedback circuit to our loudspeaker and collected pertinent testing data. While this data was not perfect due to noise within the circuit we are able to see the effects of the feedback circuit on the frequency response of the loudspeaker and get velocity and acceleration responses that we were looking for.

Contents

1. Introduction

A dynamic loudspeaker is a loudspeaker that converts an electrical signal into mechanical motion to produce sound. When an audio signal is applied to the loudspeaker's voice coil, which is suspended between the poles of a magnet, a magnetic force is generated, causing the loudspeaker's diaphragm, which is attached to the coil former around which the voice coil is wound, to vibrate and generate sound [1]. Figure 1 shows a cross-section of a dynamic loudspeaker.

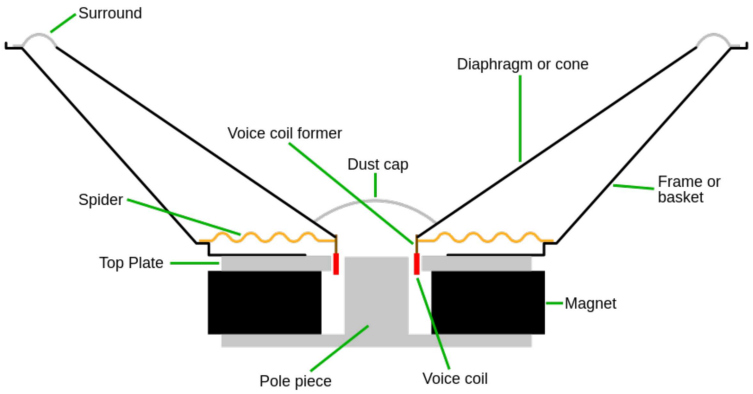

Figure 1: Cross section of a dynamic loudspeaker [2]

When a subwoofer, a loudspeaker that reproduces audio at lower frequencies, is mounted in an open baffle cabinet, i.e., a box without a back panel, its parameters are essentially the same as they would be if the subwoofer were suspended in free space. In particular, the total quality factor and the resonant frequency are unaltered by the open baffle cabinet. Because the total quality factor of an unmounted subwoofer driver is small, the frequency above which the driver has significant output is too high to be useful even though the resonant frequency is low.

A motional feedback circuit can be implemented to resolve this issue. A motional feedback loop accepts a voltage that is proportional to the acceleration of the loudspeaker's cone, integrates it to yield a voltage proportional to the loudspeaker's velocity, and then uses both the acceleration feedback and velocity feedback to adjust both the quality and the resonant frequency of the system. This results in a cone acceleration frequency response with a useful output

over a much more practical frequency range. The acceleration of the cone is particularly important because the on-axis sound pressure level is directly proportional to the acceleration of the cone [3].

2. Description of Work

To change the characteristic of our subwoofer mounted in an open baffle, we implemented a motional feedback circuit to introduce both velocity and acceleration feedback. Our feedback loop accepts an output from an accelerometer mounted to a 3D printed plug that we inserted into the coil former of the loudspeaker. This accelerometer outputs a voltage that is proportional to the acceleration of the cone. By utilizing an integrator circuit, a voltage proportional to the cone's velocity is also obtained and the feedback circuit ultimately compares the cone's acceleration and velocity to the original line-level signal to produce a corrected signal that is then applied to the audio amplifier. By altering the acceleration feedback of the system, we are able to lower the resonant frequency of the system while also increasing the quality factor. Adjusting the velocity feedback allows us to change only the quality factor and tune it to an acceptable value and thus obtain a flat frequency response within a practical frequency range.

2.1. Exploration of a Current-Driven Loudspeaker

Initially, while attempting to implement a motional feedback circuit we also investigated the potential advantages of implementing a current amplifier over a conventional voltage amplifier do drive our loudspeaker, a 10" subwoofer with a free air resonant frequency of 20 Hz. In order to determine how the current driven design affected the mechanical model of our system, we derived a transfer function to relate the velocity and acceleration of the loudspeaker's cone to the current in the voice coil. The dynamic loudspeaker can be modeled as a mechanical system consisting of masses, springs, and dampers as can be seen in Figure 2 [4]. A list of variables used in the development of the transfer functions is given in Table 1.

The motion of this system can be described by a linear second order system:

$$M\ddot{x} + D\dot{x} + Kx = f_e = Bli. \tag{1}$$

Table 1: A list of variables used in the transfer function development

Variable	Units	Description
B	$\frac{Wb}{m}$	Radial Component of Magnetic Flux Density in Magnetic Gap
D	$\frac{N-s}{m}$	Damping
f_e	N	Driving Force Due to Coil and Magnet
i	A	Current in Coil
K	$\frac{N}{m}$	Spring Constant
l	m	Total Length of Wire in Coil
x	m	Displacement of the Cone
M	kg	Mass of the Driver Diaphragm

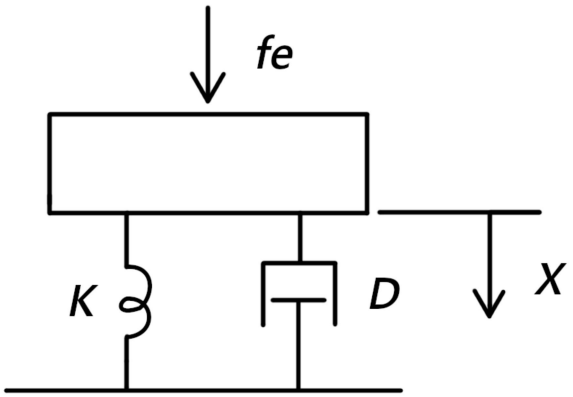

Figure 2: Diagram showing the mechanical system used to model the loudspeaker.

Expressed in the Laplace domain, (1) becomes

$$MXs^2 + DXs + KX = BlI. \tag{2}$$

Since velocity is the first derivative of displacement with respect to time, and since acceleration is the second derivative of displacement with respect to time as well as the first derivative of velocity with respect to time, from (2) we can write the following two equations:

$$BlI = MA(s) + \frac{1}{s}DA(s) + \frac{1}{s^2}KA(s) \tag{3a}$$

and

$$BlI = MsU(s) + DU(s) + \frac{1}{s}KU(s) \tag{3b}$$

where A(s) and U(s) are Laplace domain representations of the system's acceleration and velocity, respectively. Finally, we get the following two transfer functions:

$$\frac{U(s)}{I} = \frac{Bl}{Ms + K + \frac{D}{s}} \tag{4a}$$

$$\frac{A(s)}{I} = \frac{Bl}{M + \frac{K}{s} + \frac{D}{s^2}} \tag{4b}$$

The voice coil is typically modeled as a series circuit comprised of a resistance, R_E, an inductance, L_E, and a dependant voltage source to model the back electromotive force induced by the movement of the coil in the magnetic field, $Bl\frac{dx}{dt}$, as can be seen in Figure 3. However, (4a) and (4b) do not include any of these electrical impedances of the voice coil, only the mechanical impedances used to model the system. Therefore the current driven design is able to circumvent the electrical impedances of the voice coil, as they are eliminated from current-to-velocity and current-to-acceleration transfer functions entirely [5]. However, for the scope of this project, the use of a current driven design was not found to be particularly advantageous to the extent that it is worth implementing over the voltage driven design. Since the complex impedance of an inductor is represented as $Z_L = j\omega L$, where L is the inductance and ω is the angular frequency, the impedance of the inductor in this model really only presents a problem at a higher range of frequencies beyond which our subwoofer loudspeaker is intended to be operated at. Moreover, any challenges that the DC resistance might present will be corrected by the motional feedback circuit. Therefore, since the current amplifier offers no discernable advantage over the voltage amplifier, constructing our own transconductance amplifier for a motional feedback loudspeaker was not deemed to be a worthwhile endeavour and we opted for the voltage amplifier instead.

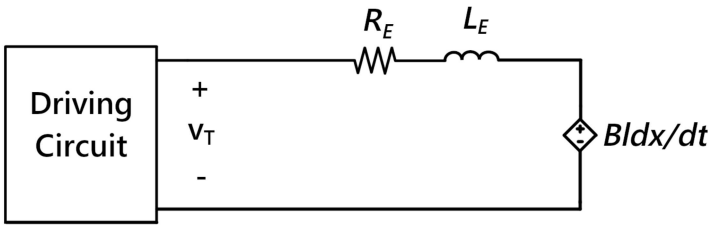

Figure 3: Circuit used to model impedance of the loudspeaker's voice coil.

2.2. The Open Baffle Cabinet

One novel design option we chose to pursue on this project was the mounting of our loudspeaker to an open baffle cabinet. According to engineer and loudspeaker expert Siegfried Linkwitz, open baffle designs present a number of benefits compared to conventional closed box cabinets that make this option worth exploring. He argued that open baffle designs can reproduce bass with less room interaction (and are thus more articulate than speakers in enclosed cabinets), circumvent issues of delayed radiation through cone and enclosure panels that are present in box speakers, and are less subject to room response if the speaker has a well-behaved polar response. In general, opting for an open baffle cabinet is believed to be a low-risk choice as it is considered difficult to poorly fabricate this design in such a way that it performs worse than a typical box speaker [3].

2.3. The Motional Feedback Circuit

The motional feedback circuit used for this project was meant to realize the transfer function of the block diagram in Figure 4. A derivation of the cone-acceleration-to-input-voltage transfer function is given below with a list of variables provided in Table 2.

From Figure 4, we can derive the transfer function $\frac{A(s)}{V_I}$ beginning with

$$A(s) = G_P D(s) H_L(s) \tag{5}$$

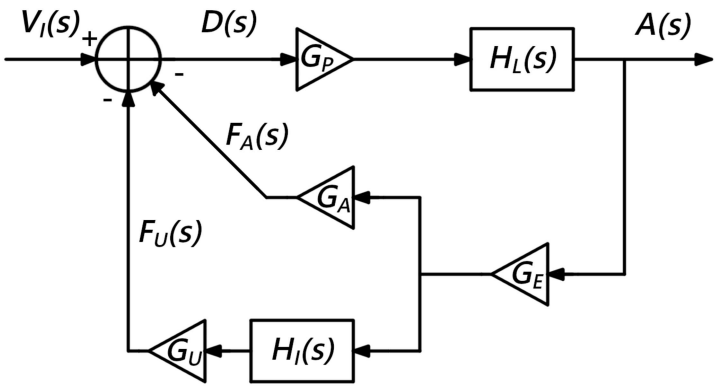

Figure 4: Block Diagram of Motional Feedback Loudspeaker System.

Table 2: A list of variables used in the transfer function development

Variable	Description
A(s)	Cone Acceleration
$V_I(s)$	Line Level Voltage
$F_A(s)$	Voltage Proportional to Cone Acceleration
$F_U(s)$	Voltage Proportional to Cone Velocity
$H_L(s)$	Cone Acceleration to Terminal Voltage Transfer Function
$H_I(s)$	Integrator Transfer Function
G_I	Integrator Gain
G_P	Gain of Power Amplifier
G_E	Gain of Accelerometer Interface
G_A	Gain of Acceleration
G_U	Gain of Velocity

where

$$D(s) = V_I(s) - F_U(s) - F_A(s). \tag{6}$$

From Figure 4,

$$F_A(s) = G_A G_E A(s) \tag{7a}$$

and

$$F_U(s) = G_U G_E H_I(s) A(s). \tag{7b}$$

By substituting (7a) and 7b into (6), we arrive at the following expression:

$$D(s) = V_I(s) - G_U G_E H_I(s) A(s) - G_A G_E A(s). \tag{8}$$

Lastly, by substituting (8) into (5), we get

$$A(s) = G_P H_L(s)[V_I(s) - G_U G_E H_I(s) A(s) - G_A G_E A(s)],$$

$$A(s) = G_P H_L(s) V_I(s) - G_P H_L(s) A(s)[G_U G_E H_I(s) + G_A G_E],$$

$$A(s) + G_P H_L(s) A(s)[G_U G_E H_I(s) + G_A G_E] = G_P H_L(s) V_I(s),$$

$$A(s)[1 + G_P G_U G_E H_L(s) H_I(s) + G_P G_L G_A G_E H_L(s)] = V_I(s)[G_P H_L(s)],$$

so that

$$\frac{A(s)}{V_I(s)} = \frac{G_P H_L(s)}{1 + G_P G_E G_U H_L(s) H_I(s) + G_P G_A G_E H_L(s)}. \tag{9}$$

Because integration in the time domain corresponds with the multiplier $\frac{1}{s}$ in the Laplace domain, we know that for the integrator circuit in the block diagram,

$$H_I(s) = \frac{G_I}{s} \tag{10}$$

where G_I is the gain of the integrator circuit. The derivation of $H_L(s)$ assumes negligible inductance effects of the voice coil and begins with with (2):

$$MXs^2 + DXs + KX = BlI.$$

Then by algebraically rearranging this equation, we arrive at an expression for the loudspeaker's cone position in terms

of the loudspeaker's mechanical parameters and the current through the voice coil:

$$X = \frac{I}{\frac{M}{Bl}s^2 + \frac{D}{Bl}s + \frac{K}{Bl}}. \tag{11}$$

By observing Figure 3, we can then write a KVL equation to express the voltage across the voice coil, or terminal voltage v_T, as follows:

$$v_T = iR_E + L_E\frac{di}{dt} + Bl\frac{dx}{dt}. \tag{12}$$

And in the Laplace domain with L_E set to 0, we see that

$$V_T = IR_E + BlXs. \tag{13}$$

Since we can express the impedance observed looking into the voice coil as the ratio of the terminal voltage to voice coil current, we can substitute (11) into (13) and arrive at the following expression:

$$Z = \frac{V_T}{I} = R_E + \frac{Bls}{\frac{M}{Bl}s^2 + \frac{D}{Bl}s + \frac{K}{Bl}} \tag{14}$$

. (14) describes a circuit characterized by two series impedances: the impedance of the coil's DC resistance, R_E, and a mechanical impedance that we will call Z_M, where

$$Z_M = \frac{1}{\frac{Ms}{(Bl)^2} + \frac{D}{(Bl)^2} + \frac{K}{(bl)^2 s}} \tag{15}$$

and Z_M can further be modeled as three parallel impedances, Z_{C_M}, Z_{R_M}, and Z_{L_M}, where

$$Z_M = \frac{1}{\frac{1}{Z_{C_M}} + \frac{1}{Z_{R_M}} + \frac{1}{Z_{L_M}}} \tag{16}$$

and

$$Z_{C_M} = \frac{(Bl)^2}{Ms}, \tag{17a}$$

$$Z_{R_M} = \frac{(Bl)^2}{D}, \tag{17b}$$

$$Z_{L_M} = \frac{(Bl)^2 s}{K}. \tag{17c}$$

Therefore, the mechanical impedance of the loudspeaker can be modeled as a parallel connection of a capacitor C_M, a resistor R_M, and an inductor L_M as in Figure 5 where

$$C_M = \frac{M}{(Bl)^2}, \tag{18a}$$

$$R_M = \frac{(Bl)^2}{D}, \tag{18b}$$

and

$$L_M = \frac{(Bl)^2}{K}. \tag{18c}$$

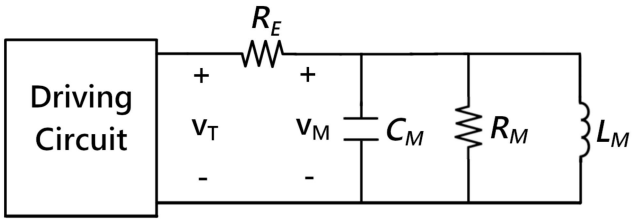

Figure 5: Circuit used to model electrical impedance of the loudspeaker's voice coil and cone's mechanical impedance.

With the mechanical impedance Z_M reflected across the dependent voltage source used in the voice coil model, we

can now use voltage division to express V_M in terms of V_T:

$$V_M = V_T \frac{Z_M}{R_E + Z_M}$$

$$\frac{V_M}{V_T} = \frac{Z_M}{R_E + Z_M}. \tag{19}$$

From Figure 3 we can see that v_M is the same as $\mathrm{Bl}\frac{dx}{dt}$, so in the Laplace domain, we are able to arrive at the following three relations:

$$V_M = BlsX, \tag{20a}$$

$$V_M = BlU, \tag{20b}$$

and

$$V_M = \frac{BlA}{s} \tag{20c}$$

where U is the veloctiy of the cone and A is the acceleration of the cone. By substituting (20b) into (19), we are able develop a cone-acceleration-to-terminal-voltage transfer function:

$$\frac{BlA}{sV_T} = \frac{Z_M}{R_E + Z_M}$$

$$\frac{A}{V_T} = \frac{s}{Bl} \frac{Z_M}{R_E + Z_M} \tag{21}$$

From here, we will algebraically manipulate this transfer function in order to ultimately express it in terms of the loudspeaker's resonanant frequency ω_s, its electrical quality Q_{ES}, and its total quality Q_{TS}, beginning by manipulating the voltage divider $\frac{Z_M}{R_E+Z_M}$:

$$
\begin{aligned}
\frac{Z_M}{R_E+Z_M} &= \frac{(\frac{1}{Z_{C_M}}+\frac{1}{Z_{R_M}}+\frac{1}{Z_{L_M}})^{-1}}{R_E+(\frac{1}{Z_{C_M}}+\frac{1}{Z_{R_M}}+\frac{1}{Z_{L_M}})^{-1}} \\
&= \frac{1}{R_E(\frac{1}{Z_{C_M}}+\frac{1}{Z_{R_M}}+\frac{1}{Z_{L_M}})+1} \\
&= \frac{1}{R_E(sC_M+\frac{1}{R_M}+\frac{1}{sL_M})+1} \\
&= \frac{s}{R_EC_Ms^2+\frac{R_E}{R_M}s+\frac{R_E}{L_M}+s} \\
&= \frac{s\frac{1}{R_EC_M}}{s^2+\frac{1}{R_EC_M}(\frac{R_E}{R_M}+1)s+\frac{1}{L_MC_M}} \\
&= \frac{s\frac{1}{R_EC_M}}{s^2+\frac{1}{C_M}(\frac{1}{R_M}+\frac{1}{R_E})s+\frac{1}{L_MC_M}}
\end{aligned}
$$

$$
\frac{Z_M}{R_E+Z_M} = \frac{s\frac{1}{R_EC_M}}{s^2+\frac{1}{C_M}\frac{1}{R_E||R_M}s+\frac{1}{L_MC_M}}. \tag{22}
$$

Before we can substitute (22) into (21), we can first use the following expressions for ω_s, Q_{ES}, and Q_{TS}:

$$
\omega_s = \frac{1}{\sqrt{L_MC_M}}, \tag{23a}
$$

$$
Q_{ES} = R_E\sqrt{\frac{C_M}{L_M}}, \tag{23b}
$$

and

$$
Q_{TS} = (R_E||R_M)\sqrt{\frac{C_M}{L_M}}. \tag{23c}
$$

By further manipulating (23a), (23b), and (23c), we arrive at the following relations:

$$
\omega_s^2 = \frac{1}{L_MC_M}, \tag{24a}
$$

$$
\frac{\omega_s}{Q_{ES}} = \frac{1}{R_EC_M}, \tag{24b}
$$

and

$$\frac{\omega_s}{Q_{TS}} = \frac{1}{C_M(R_E||R_M)}. \tag{24c}$$

By substituting (24a), (24b), and (24c) into (22), we see that

$$\frac{Z_M}{R_E + Z_M} = \frac{\frac{\omega_s}{Q_{ES}}s}{s^2 + \frac{\omega_s}{Q_{TS}}s + \omega_s^2}. \tag{25}$$

Finally, by substituting (25) into (21), we arrive at a transfer function for $H_L(S)$:

$$\frac{A}{V_T} = H_L(s) = \underbrace{\left(\frac{1}{Bl}\frac{\omega_s}{Q_{ES}}\right)}_{G_L}\frac{s^2}{s^2 + \frac{\omega_s}{Q_{TS}}s + \omega_s^2}. \tag{26}$$

At last we can substitute (26) and (10) into (9) and begin to investigate how the motional feedback circuit will affect both the quality and the resonant frequency of the system:

$$\begin{aligned}
\frac{A}{V_I} &= G_L\frac{G_P\left(\frac{s^2}{s^2+\frac{\omega_s}{Q_{TS}}s+\omega_s^2}\right)}{1 + G_PG_EG_UG_IG_L\left(\frac{s}{s^2+\frac{\omega_s}{Q_{TS}}s+\omega_s^2}\right) + G_PG_AG_EG_L} \\
&= G_L\frac{G_Ps^2}{s^2 + s\frac{\omega_s}{Q_{TS}} + \omega_s^2 + G_PG_EG_UG_IG_Ls + G_PG_AG_LG_Es^2} \\
&= G_L\frac{G_Ps^2}{s^2(1 + G_PG_AG_LG_E) + s\left(\frac{\omega_s}{Q_{TS}} + G_PG_EG_UG_IG_L\right) + \omega_s^2}
\end{aligned}$$

$$\frac{A}{V_I} = \frac{G_PG_L}{1 + G_PG_AG_LG_E}\left[\frac{s^2}{s^2 + s\left(\frac{\frac{\omega_s}{Q_{TS}} + G_PG_EG_UG_IG_L}{1+G_PG_AG_LG_E}\right) + \frac{\omega_s^2}{1+G_PG_AG_LG_E}}\right]. \tag{27}$$

From here, we will establish variables G_X and ω_o as follows:

$$G_X = G_PG_LG_E \tag{28}$$

and

$$\omega_o = \frac{\omega_s}{\sqrt{1+G_P G_A G_L G_E}} = \frac{\omega_s}{\sqrt{1+G_X G_A}}. \tag{29}$$

Furthermore, let

$$\frac{Q}{\omega_o} = \frac{1+G_P G_A G_L G_E}{\frac{\omega_s}{Q_{TS}} + G_P G_E G_U G_I G_L} = \frac{1+G_A G_X}{\frac{\omega_s}{Q_{TS}} + G_U G_I G_X} \tag{30}$$

Developing (30) further and by substituting in (29) for ω_o, we see that

$$Q = \frac{\omega_s \sqrt{1+G_X G_A}}{\frac{\omega_s}{Q_{TS}} + G_X G_I G_U}$$

$$Q = \frac{Q_{TS}\sqrt{1+G_X G_A}}{1+\frac{Q_{TS}}{\omega_s} G_X G_I G_U}. \tag{31}$$

From (29), (30), and (28) we can rewrite (27) as

$$\frac{A}{V_I} = \frac{G_P G_L}{1+G_X G_A}\left[\frac{s^2}{s^2 + s\frac{\omega_o}{Q} + \omega_o^2}\right]. \tag{32}$$

By inspecting (29) and (31), it is apparent how adjusting gains in the feedback circuit can affect both Q and ω_o. Specifically, G_A and G_U will be the particular gains to be adjusted using potentiometers in order to alter the resonant frequency and quality of the loudspeaker. A circuit of the feedback loop in the block diagram in Figure 4 is given in Figure 6.

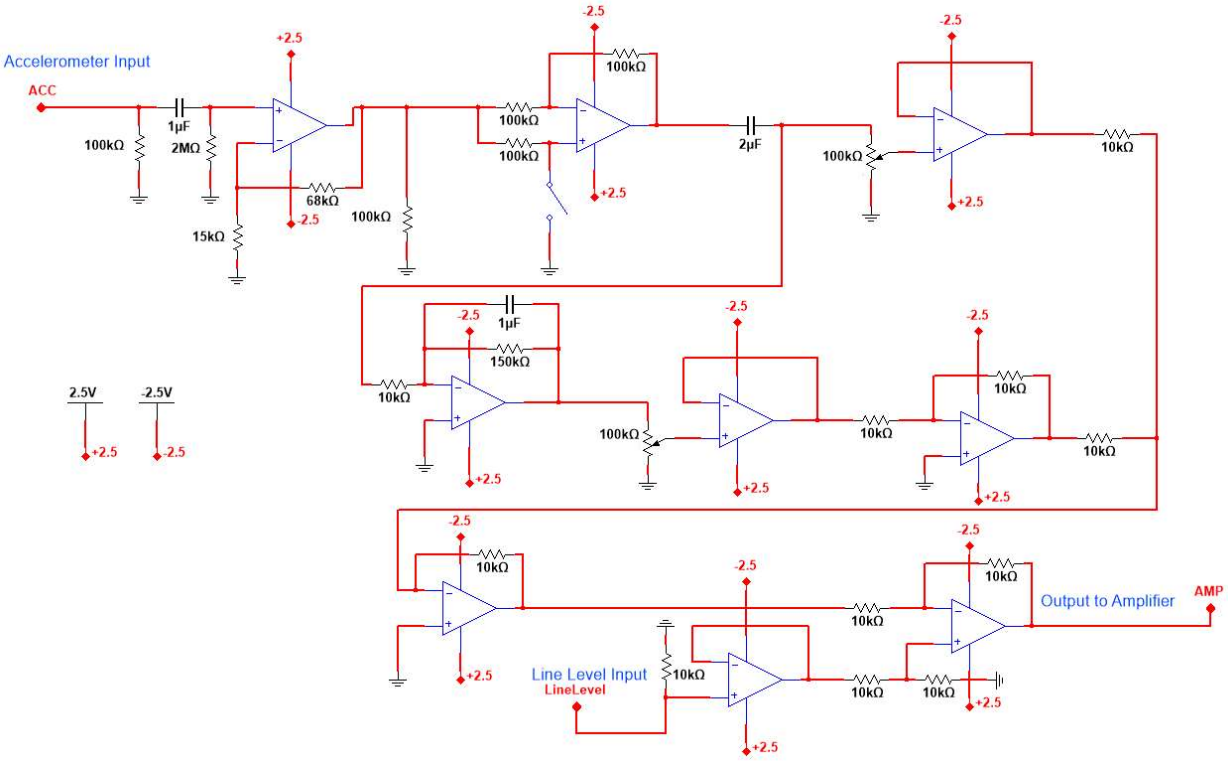

Figure 6: The Motional Feedback Circuit

2.3.1. *The Power Supply*

Our board was powered by a 9V battery-to-barrel-jack adapter, a voltage regulator, and a rail splitter that ultimately led to rail voltages of V_{CC}^{+}=+5.0V and V_{CC}^{-}=0V, i.e., V_{CC}^{-} was grounded. The rail voltages were used to power each op amp as well as the digital potentiometers in our feedback circuit. Signal ground was set to +2.5V. The KiCAD schematic for our power supply can be seen in Figure 7 where U3 is the voltage regulator and U4 is the rail splitter. A switch was added to the power supply so the circuit could effectively be turned on and off and is represented by U2 in Figure 7. A light-emitting diode (labeled LED1) was also included so that we could visibly determine whether the power supply was turned on or off.

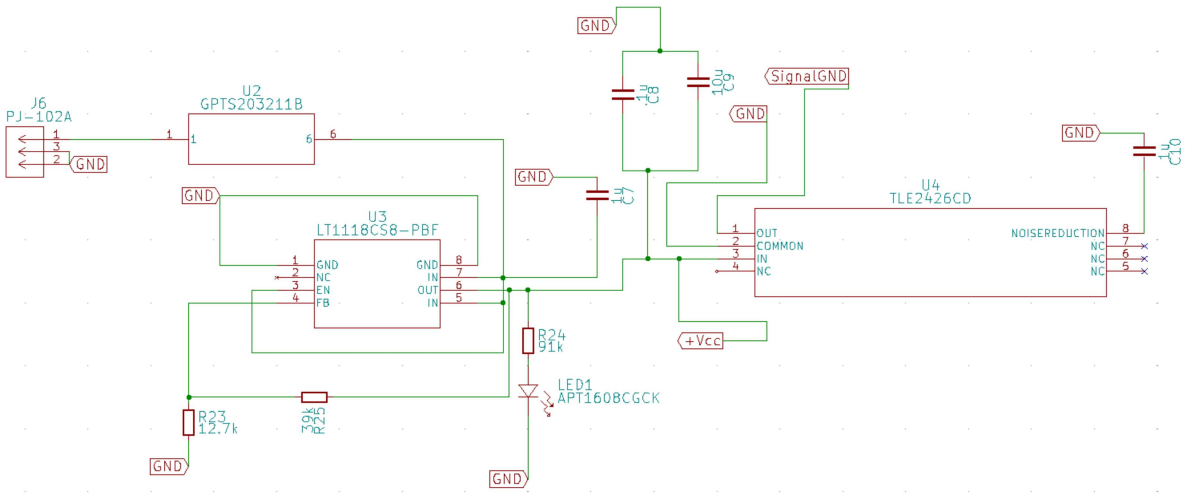

Figure 7: The power supply

2.3.2. *The Accelerometer Interface*

The accelerometer interface is the part of the circuit that receives the signal produced by the accelerometer. After the signal is received it is sent through a filter to reduce any noise from the signal. The signal is then amplified before going through the feedback circuit.

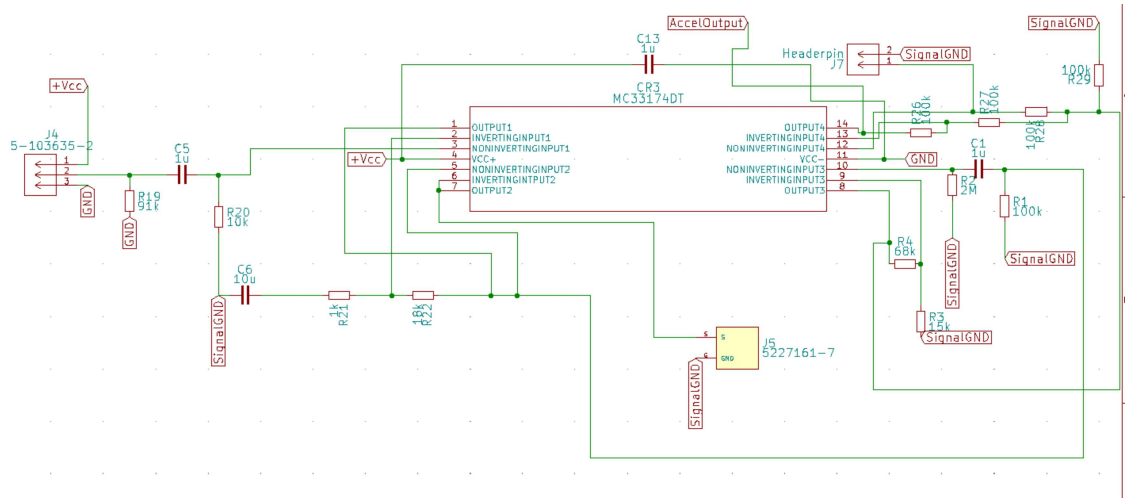

Figure 8: The accelerometer interface

2.3.3. The Switching Inverter

Depending on how the accelerometer is mounted, the signal it produces may inherently be inverted. Due to the potential for this unwanted inversion, the inverting op-amp in Figure 9 was introduced into the feedback circuit. This inverter can be "switched" on and off, so when the switch is closed, it functions as an inverter but will otherwise function as a unity gain amplifier when the switch is open, thus leaving the signal unchanged.

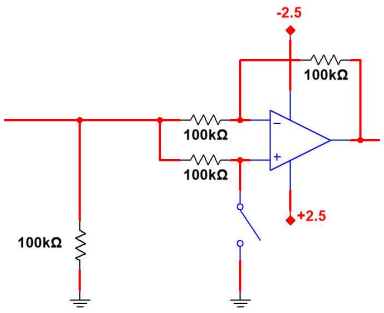

Figure 9: The switchable inverting amplifier

2.3.4. *The Acceleration Branch*

Because the voltage output of the accelerometer is already proportional to cone's acceleration, this signal does need to be operated on. The buffer in Figure 10 However, in order to adjust the resonant frequency and the quality of the system, we can adjust the digital potentiometer to affect the gain G_A such that:

$$0 \leq G_A \leq 1. \tag{33}$$

Understanding the range of G_A, we can inspect (29) to determine the range of ω_o to be:

$$\frac{\omega_s}{\sqrt{1+G_X}} \leq \omega_o \leq \omega_s. \tag{34}$$

Thus, we are able to lower the resonant frequency of the system as needed by adjusting the potentiometer, which in turn adjusts the gain G_A.

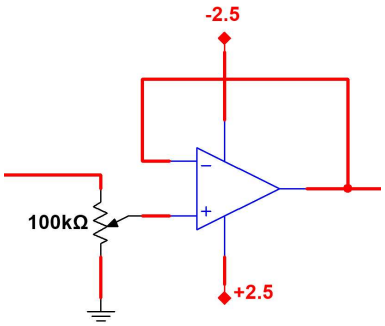

Figure 10: Acceleration branch comprised of a potentiometer and buffer amplifier.

2.3.5. *The Velocity Branch*

Since the voltage output of the accelerometer is proportional to the cone's acceleration, if we are to procure some $F_U(s)$ as shown in 4, we must branch off from the acceleration signal path through an integrator to obtain a voltage that is proportional to the cone's velocity. The node connected to the output of the switchable inverter depicted in Figure 9 runs to the input of an integrator circuit, as can be seen in Figure 11, which has the previously established

transfer function of

$$H_I(s) = \frac{G_I}{s}$$

where

$$G_I = -\frac{1}{RC}. \tag{35}$$

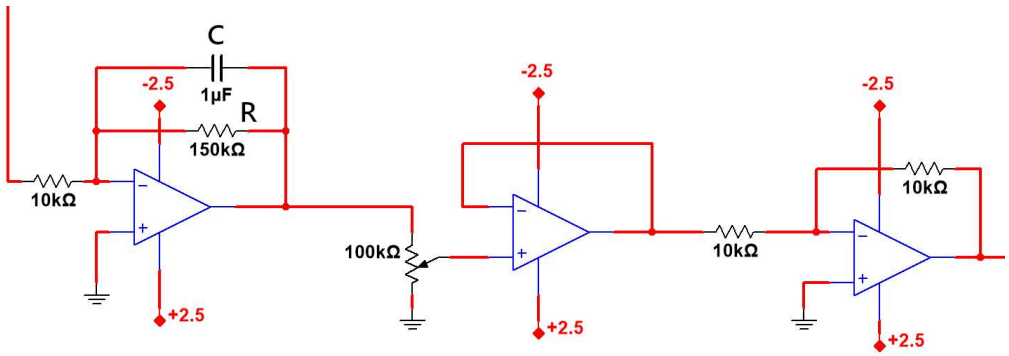

Figure 11: Velocity branch comprised of an integrator, a [potentiometer/buffer circuit, and an inverter.

From here, a voltage proportional to the cone velocity is obtained and then run through the second half of the velocity circuit to characterize G_U in 4. G_U is realized in this circuit in the form of a buffer op-amp cascaded with an inverting amplifier with a gain of -1. The gain G_U can be altered by adjusting the potentiometer such that

$$-1 \leq G_U \leq 0 \tag{36}$$

and

$$0 \leq G_U H_L(s) \leq \frac{1}{sRC}. \tag{37}$$

Furthermore, in the same way that we evaluated how altering G_A affected the resonant frequency of the system, we can likewise develop an understanding for how adjusting G_U and G_A (and by extension, ω_o will affect the system's quality, which becomes apparent by inspecting (31) within the context of these changing parameters.

2.3.6. The Summing Amplifier

In order to realize (6), a summing amplifier and a difference amplifier were implemented in cascade to first sum $F_U(s)$ and $F_A(s)$ and then subtract that from the line level input $V_I(s)$. The inverting amplifier in 12 scales $V_{F_A(s)}$ and $V_{F_U(s)}$ by $\frac{R_f}{R_{F_A}}$ and $\frac{R_f}{R_{F_U}}$, respectively, and adds them such that

$$V_{D(s)} = -\left(\frac{R_f}{R_{F_A}} V_{F_A(s)} + \frac{R_f}{R_{F_U}} V_{F_U(s)}\right) \tag{38}$$

And since R_f=R_{F_A}=R_{F_U}, (12) can be further reduced to

$$V_{out}(s) = -(V_{F_A(s)} + V_{F_U(s)}). \tag{39}$$

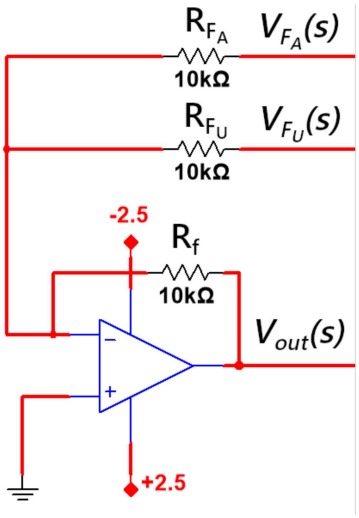

Figure 12: Voltage summing amplifier

Note that this operation results in an inversion of the sum of $V_{F_A(s)}$ and $V_{F_U(s)}$. Because of this, it then follows that $V_{F_A(s)}$ and $V_{F_U(s)}$ must be inverted with respect to $F_A(s)$ and $F_U(S)$, respectively such that

$$F_A(s) = -V_{F_A(s)} \tag{40a}$$

and

$$F_U(s) = -V_{F_U(s)}. \tag{40b}$$

Since this summing amplifier will always invert the output, it is necessary that the relations in (40a) and (40b) are taken into account when considering the operation of the switching inverter in Figure 9. If the accelerometer is mounted in such a way that it outputs in inverted voltage proportional to the cone's acceleration, then the switch must remain closed so that the switchable inverter acts only as a buffer and the inversion of the signal is preserved. However if the accelerometer is mounted in such a way that it outputs a non-inverted voltage proportional to the cone's acceleration, the switch must open so that the signal may be properly inverted. Ultimately, there must be be an inverted signal at the ouput of the switchable inverter, whether this be achieved through opening the switch or mounting the accelerometer in a particular fashion so that (6) may be correctly obtained at the output of the summing amplifier.

2.3.7. The Difference Amplifier

Lastly, the sum of $F_A(s)$ and $F_U(s)$ must be subtracted from $V_I(s)$ to produce a signal $D(s)$. This difference can be obtained with the difference amplifier in Figure 13. This amplifier subtracts a voltage proportional to $V_{out}(s)$ from a voltage proportional to $V_I(s)$ in the following manner:

$$V_{D(s)} = \left(\frac{R_4}{R_4+R_3}\right)\left(\frac{R_1+R_2}{R_1}\right)V_I(s) - \left(\frac{R_2}{R_1}\right)V_{out}(s). \tag{41}$$

Because R_1=R_2=R_3=R_4, (41) can therefore simplify to

$$V_{D(s)} = V_I(s) - V_{out}(s). \tag{42}$$

This resulting signal is then fed back into the input of the voltage amplifier whereafter it drives the loudspeaker.

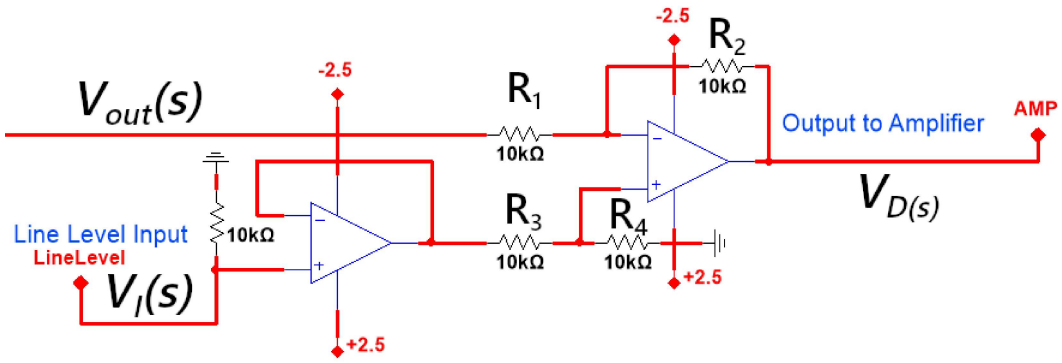

Figure 13: Voltage differential amplifier

2.3.8. Circuit Simulations

Before finalizing the design of our feedback circuit, we designed a circuit that could model our loudspeaker and simulated the acceleration response of the cone to ensure that the feedback circuit would, theoretically, work as intended.

To first verify that our design would not be adversely affected by the inductance of the voice coil, we constructed a simulation circuit to model the electronic and mechanical impedances of the loudspeaker and we were ultimately able to develop the circuit in Figure 14 that modeled the power amplifier, loudspeaker, and accelerometer.

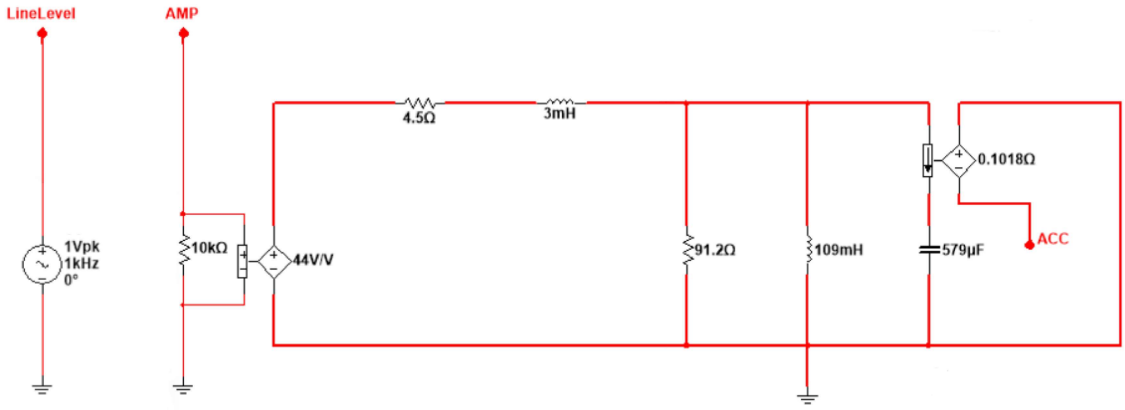

Figure 14: Simulation circuit model for the power amplifier, loudspeaker, and accelerometer

The motional feedback circuit was also incorporated into our simulations here by connecting the nodes labeled "LineLevel", "AMP", and "ACC" seen in Figure 6 to the corresponding nodes in Figure 14. Simulations were first run

with the 3mH voice coil inductance labeled "L1" shorted out to establish an expectation of results for a circuit that *does* include this inductance. As can be seen by comparing the plot in Figure 15 with the plot in Figure 16, the inductance of the voice coil only starts to affect the cone acceleration's frequency response at frequencies beyond approximately 100-200 Hz, so the voice coil's inductance was not expected to adversely affect the system.

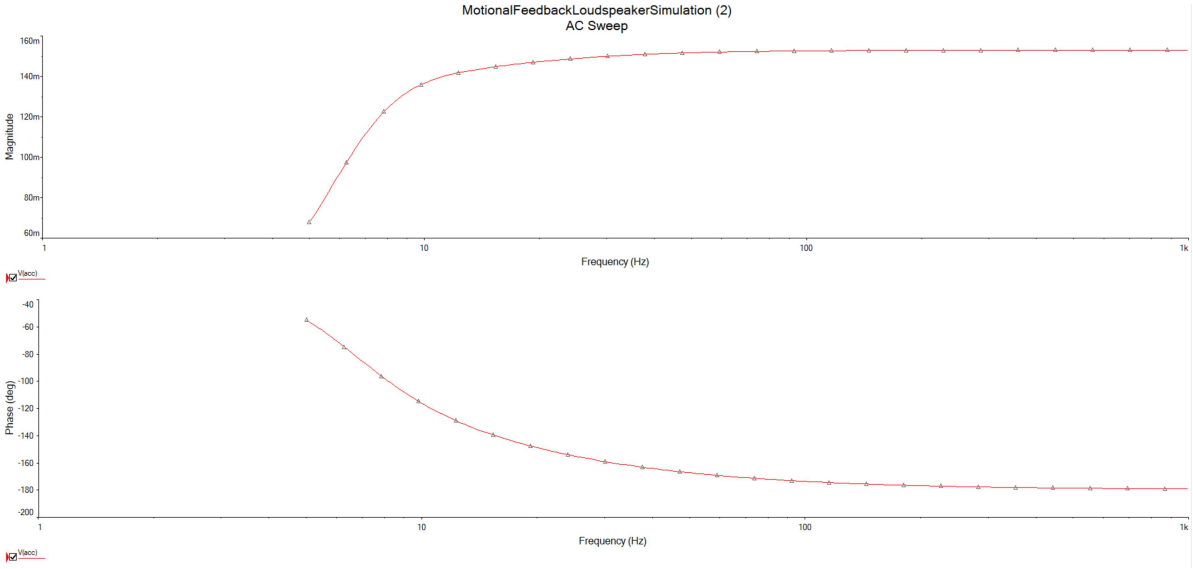

Figure 15: Acceleration frequency response with voice coil inductance neglected.

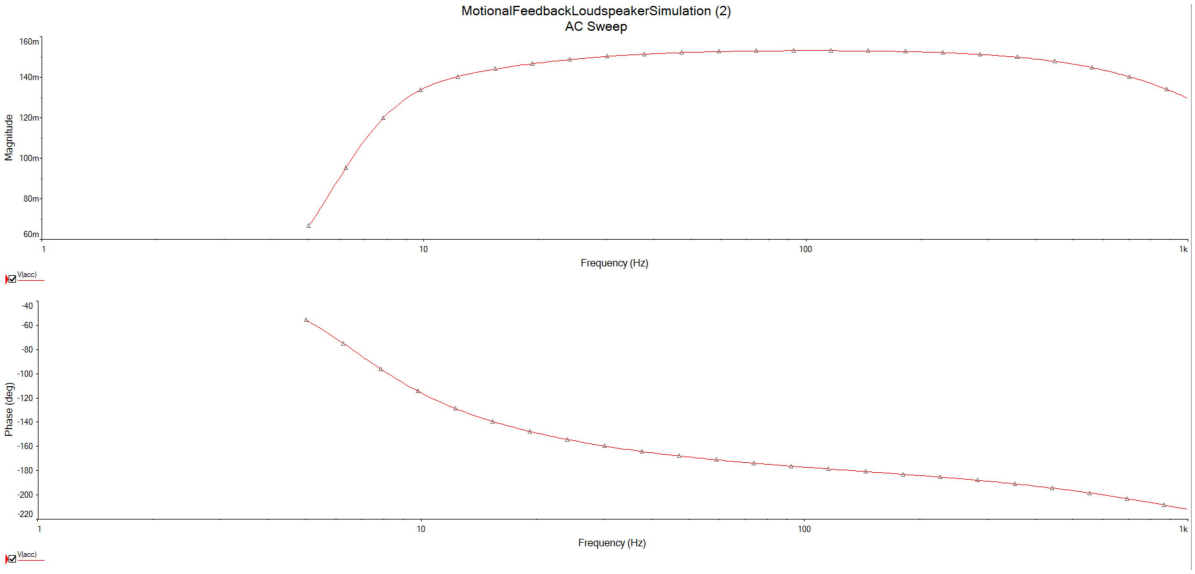

Figure 16: Acceleration frequency response with voice coil inductance included.

Having gained confidence in our loudspeaker's compatibility with the feedback circuit, we proceeded to observe

how adjusting the potentiometers would affect our simulation results. First, both potentiometers were set to 0% thereby setting G_A and G_U to 0 and effectively making ω_o=ω_s and Q=Q_{TS} in theory. We would expect that measuring the magnitude plot at the free air resonant frequency of 20Hz would yield a magnitude equal to the total Q value, or 0.31, and indeed this is what we found, as can be seen in Figure 17

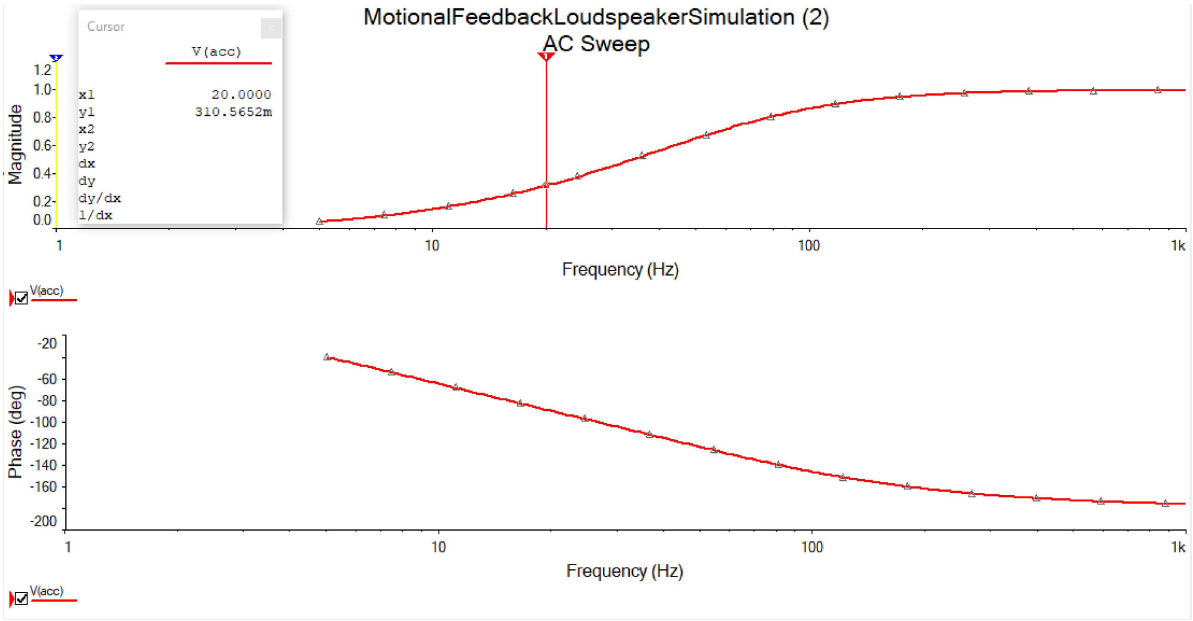

Figure 17: Acceleration Frequency response with G_A=0 and G_U=0

Then, we adjusted the potentiometers to appropriate values such that a flat frequency response similar to the ones shown in Figure 15 and Figure 16. By adjusting G_A to 1 and G_U to 0.6 after setting their corresponding potentiometers to 100% and 60%, respectively, we were indeed able to obtain a suitable frequency response as shown in 18, thus giving us confidence in the design of the motional feedback circuit.

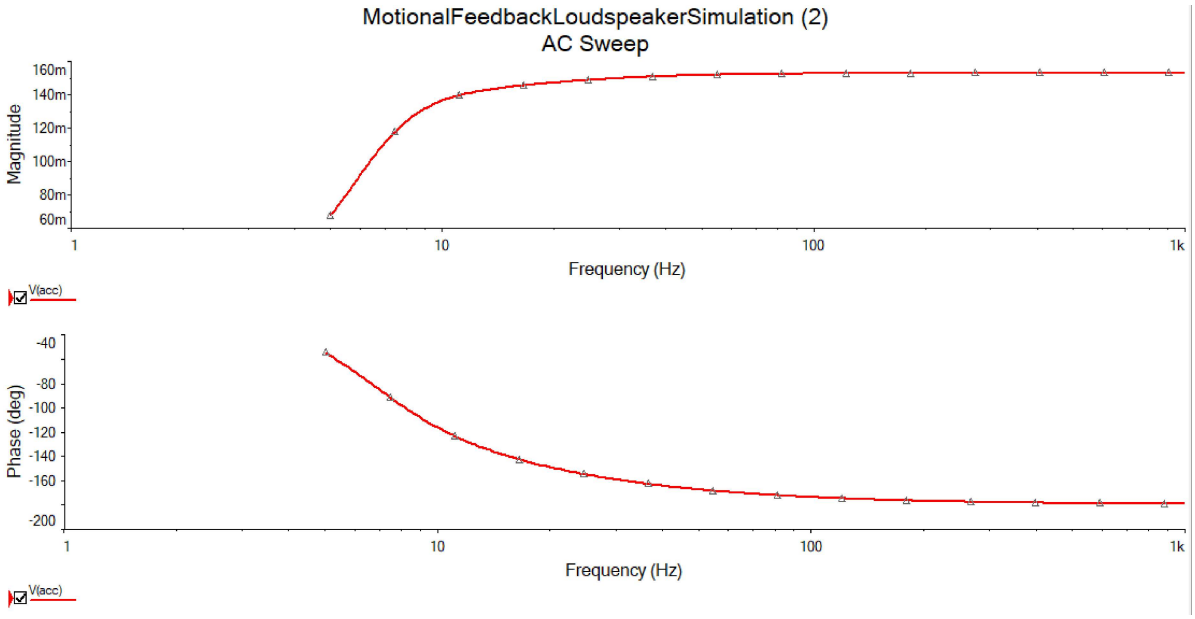

Figure 18: Acceleration frequency response with G_A=1 and G_U=0.65

3. Results and Conclusions

Having successfully obtained our simulation results, we then designed a printed circuit board so that we could implement an actual motional feedback circuit with our subwoofer. To make testing more feasible, our PCB included appropriately placed BNC jacks along the signal path such that we could measure voltages proportional to the cone's velocity and acceleration. Before we tested our circuit with the actual subwoofer, we constructed a Sallen-Key high-pass filter to model the response of the loudspeaker, voltage amplifier, and accelerometer and immediately noticed an error in the design of our printed circuit board as the connections at the inverting and non-inverting terminals of the very first op amp in the signal path (labeled "NONINVERTINGINPUT1" and "INVERTINGINPUT1" on CR3 in Figure 8) were accidentally reversed with one another in our design. Fortunately, this issue was fixed as these connections on the board were cut and new wires were soldered appropriately to make the proper connections on our circuit board.

After properly testing the PCB with the Sallen-Key model, we connected it to the loudspeaker and voltage amplifier. Initially, we ran an AC frequency sweep from 5 Hz to 100 Hz with both potentiometer wipers set to 0% (i.e., effectively eliminating the feedback altogether) and obtained plots for the cone acceleration magnitude and the cone velocity magnitude as can be seen in Figures 19 and 20. These measurements were taken with a commercially accelerometer interface rather than with our circuit, as too much noise was present without feedback to be able to obtain clean data. We expected a high pass filter and a bandpass filter for each, respectively, and indeed that is what we obtained. Note that the decibel scale's 0 reference in our plots is arbitrary and is unimportant to demonstrating the operation of our feedback circuit. Furthermore, analysis of the individual data points and observing the frequency at which the phase response crossed the x axis told us that the resonant frequency was at right about 20 Hz, which was also to be expected, seeing as this is the free air resonant frequency of our subwoofer. Equation (31) was then used to calculate the total quality factor of the system, which was found to be exactly Q_{TS}, or 0.31.

Next, we adjusted the wipers of the potentiometers using the code in Listing 1 in Appendix D and set them such that G_A=0.2 and G_U=0.2. Running an AC frequency sweep yielded the acceleration and velocity magnitude plots in Figure 21 and Figure 22. Further observing the individual data points revealed that the resonant frequency had indeed been lowered, as expected and now sat at about 17 Hz. Consulting Equation (31) once more, we find that the quality

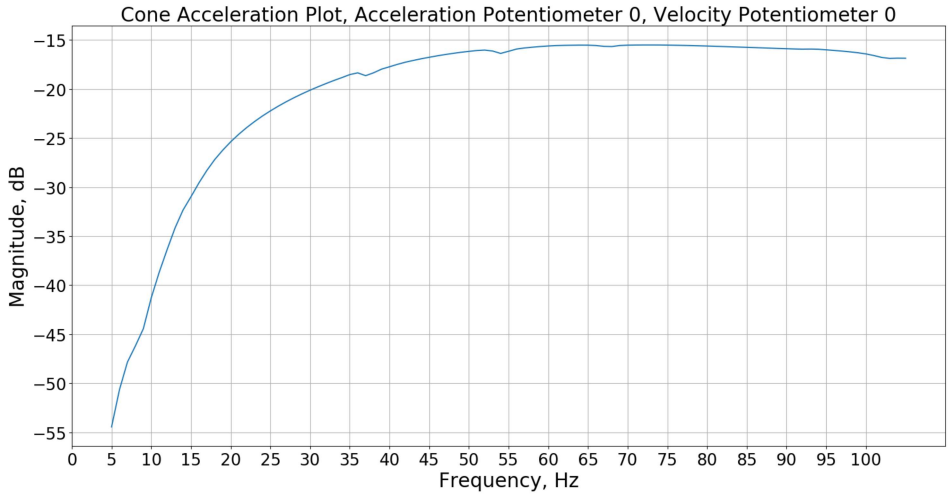

Figure 19: Acceleration magnitude response with G_A=0 and G_U=0

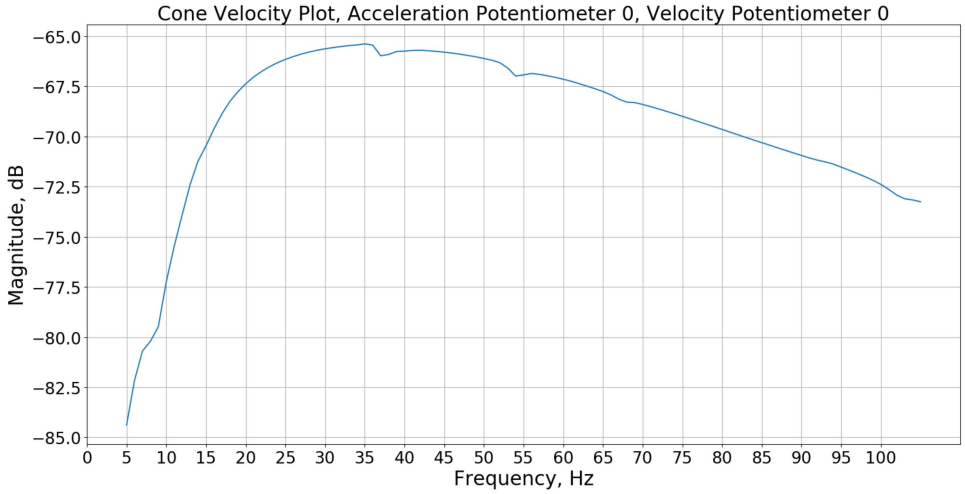

Figure 20: Velocity magnitude response with G_A=0 and G_U=0

factor, ideally, would be approximately 0.513.

Next, we set the wipers of the potentiomers such that G_a=0.59 and G_U=0.59. When we ran another AC sweep, we obtained the acceleration and velocity magnitude plots in Figures 23 and 24, respectively. By further analyzing our plots, we found that the resonant frequency had once more been lowered, this time to about 14 Hz. Conversely, Equation (31) tells us that this would ideally shift the total quality factor down to approximately 0.308.

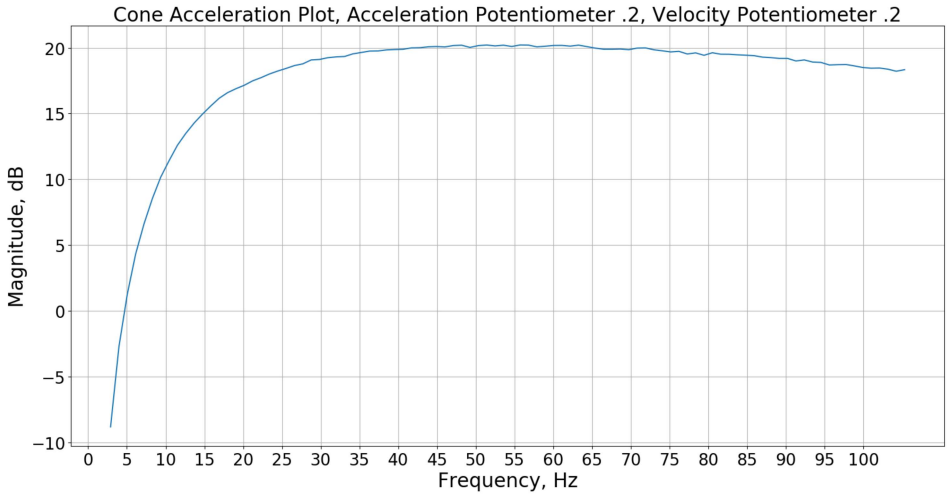

Figure 21: Acceleration magnitude response with G_A=0.2 and G_U=0.2

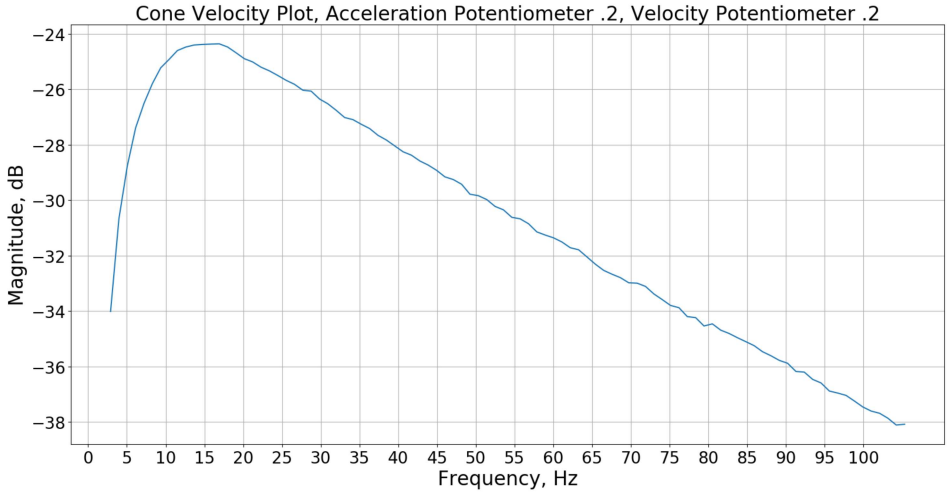

Figure 22: Velocity magnitude response with G_A=0.2 and G_U=0.2

Lastly, we set the potentiometer wipers to the "ideal" values found through trial and error in the simulations to attempt to obtain an acceleration magnitude response that resembles the plot in Figure 18. To do this, we set the potentiometers such that G_A=1 and G_U=0.65 and obtained the velocity and acceleration magnitude plots seen in Figures 25 and 26. This lowered the resonant frequency to about 15 Hz and tweaked the total quality factor to about 0.365.

From these test results we are able to draw a few different conclusions. Looking at the acceleration and velocity

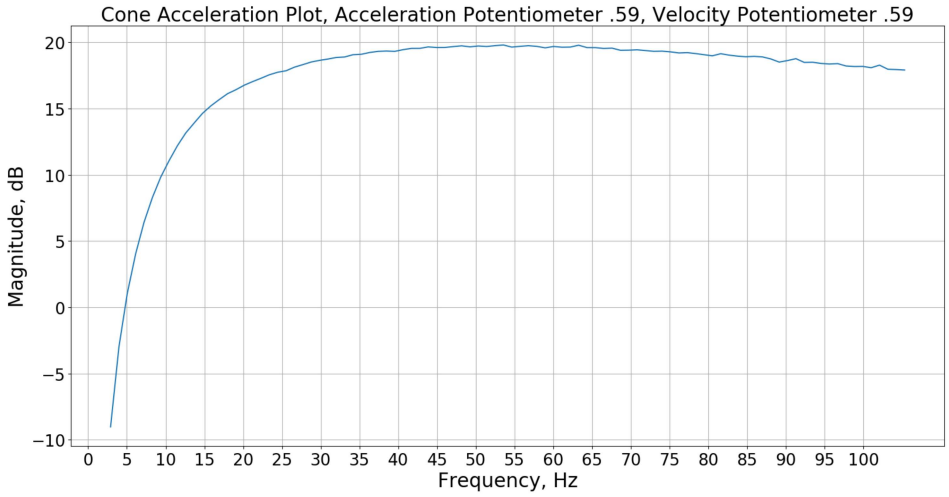

Figure 23: Acceleration magnitude response with G_A=0.59 and G_U=0.59

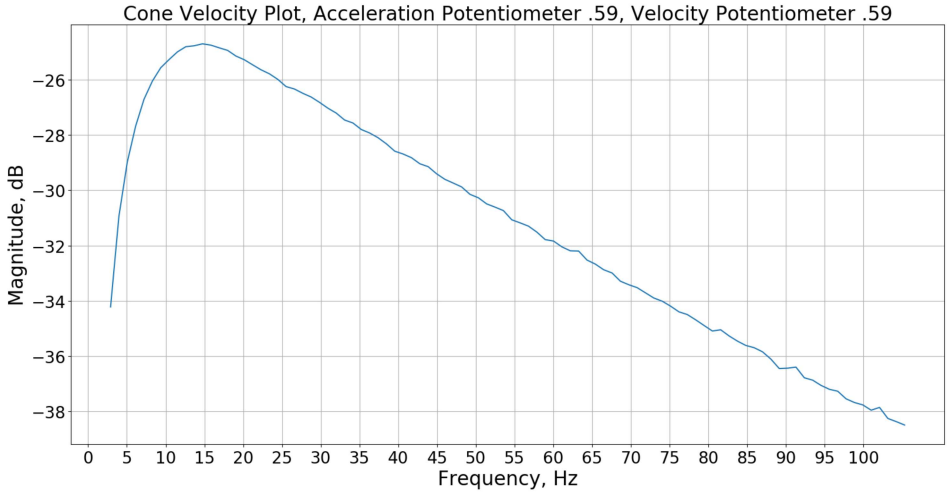

Figure 24: Velocity magnitude response with G_A=0.59 and G_U=0.59

plots it is apparent that the feedback circuit does affect the output of the loudspeaker and that it makes a significant difference. This is clearly a good result since our primary goal when we began this project was to be able to design and implement a feedback circuit that was able to affect and improve the response of the circuit. We were also able to get a nice looking bandpass filter when we look at the velocity magnitude which is what we would expect to occur there. We are also able to see a fairly flat response for the acceleration curve which is about what we would expect to obtain. Despite these improvements, however, it was difficult to truly analyze the effect the circuit had on

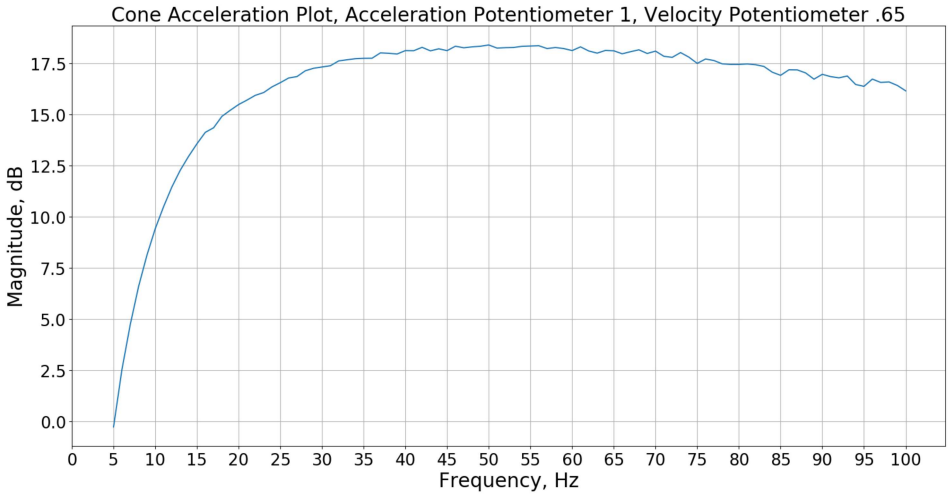

Figure 25: Acceleration magnitude response with G_A=1 and G_U=0.65

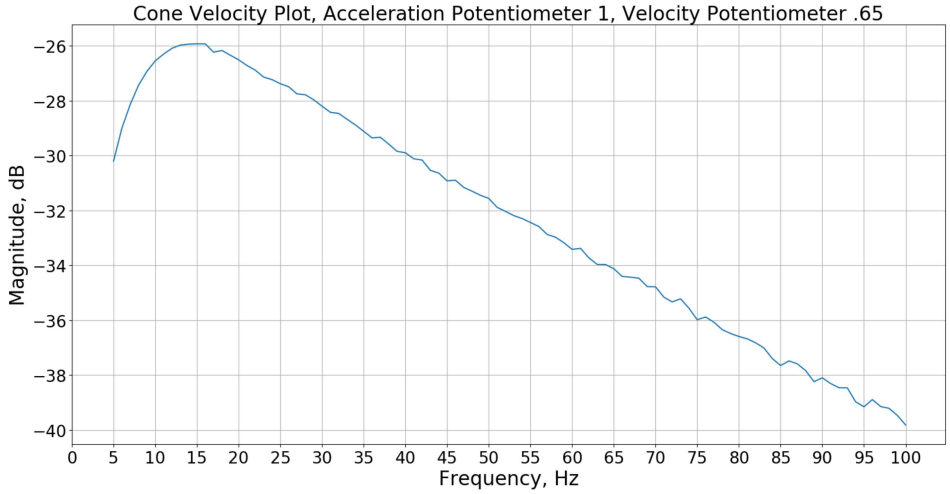

Figure 26: Velocity magnitude response with G_A=1 and G_U=0.65

the resonant frequency and quality factor of the system, as considerably noisy signals made it difficult to make any conjectures about the circuit's performance when the acceleration and velocity feedback were reduced, i.e., when both potentiometer wipers were set low. There was enough evidence however to conclude that our thesis was correct in that we successfully implemented a feedback circuit that allows for the quality factor and the resonant frequency of the loudspeaker to be adjusted such that we obtained a cone acceleration frequency response with a significant output over a useful frequency range.

There were some undesirable effects that we considered after our testing as sources of issues, particularly relating to the accelerometer and the 3D printed plug to which it was mounted. The most obvious of these was the added mass of the acceleromter and plug to the cone, which theoretically would have affected both the quality factor and the resonant requency of the system. However, the masses of these objects are considerably small, and since the motional feedback circuit was intended to adjust the system's quality factor and resonant frequency, these effects could be ignored. Secondly, we considered that the accelerometer's own frequency response could effect our circuit's performance in a way that didn't manifest in the simulation stages of this project. However, we found that the accelerometer interface sugested by the part manufacturer as well as our use of the device within its recommended frequency band of 5 Hz-10 kHz suggest that the accelerometer would not produce undesired effects.

We are also able to draw some conclusions about how we could improve the design in the future. One primary way we could improve the operation of the circuit in the future would be to reprint it with the inverting and non-inverting terminals of the very first op amp in the signal path (labeled "NONINVERTINGINPUT1" and "INVERTINGINPUT1" on CR3 in Figure 8) switched. That should be able to reduce the noise the circuit has which would improve the frequency response of the feedback circuit.

A. List of Parts for PCB

Ref Des	Value	Description	Manufacturer	Manufacturer Part Number
U1	$100k\Omega$	2 circuit digital potentiometer	Maxim Integrated	DS1803E-100+
U2	–	On\off switch	CW Industries	GPTS203211B
U3	–	Voltage Regulator	Analog Devices Inc.	LT1118CS8#PBF
U4	–	Rail Splitter	Texas Instruments	TLE2426CD
CR1, CR2, CR3	–	4 circuit op amp	STMicroelectronics	MC33174DT
R1, R26, R27, R28, R29	$100k\Omega$	Resistor	Bourns Inc.	CR0805-JW-104ELF
R2	$2M\Omega$	Resistor	Bourns Inc.	CR0805-JW-205ELF
R3	$15k\Omega$	Resistor	Bourns Inc.	CR0805-FX-1502ELF
R4	$68k\Omega$	Resistor	Bourns Inc.	CR0805-FX-6802ELF
R5, R6, R8, R9, R10, R11, R12, R13, R14, R15, R16, R17, R18, R20	$10k\Omega$	Resistor	Bourns Inc.	CR0805-JW-103ELF
R7	$150k\Omega$	Resistor	Bourns Inc.	CR0805-FX-1503ELF
R19, R23, R24, R25	$91k\Omega$	Resistor	Bourns Inc.	CR0805-FX-9102ELF
R21	$1k\Omega$	Resistor	Bourns Inc.	CR0805-JW-102ELF
R22	$18k\Omega$	Resistor	Bourns Inc.	CR0805-JW-183ELF
C1, C2, C3, C4, C7, C10, C11, C12, C13	$1\mu F$	Capacitor	Kemet	C0805C105J4RACTU
C5, C8	$0.1\mu F$	Capacitor	Kemet	C0805C104M4RAC7800
C6, C9	$10\mu F$	Capacitor	Kemet	C0805C106K4PACTU
J1, J2, J5, J8	–	BNC Jack	TE Connectivity AMP Connectors	5227161-7
J3	–	Arduino Jack	TE Connectivity AMP Connectors	282834-3
J4	–	Accelerometer Connector Header	TE Connectivity AMP Connectors	5-103635-2
J6	–	Power Jack	GlobTek Inc.	JACK-C-PC-10A-RA(R)
J7	–	Header Pin	Würth Elektronik	61300211121
LED1	–	LED	Kingbright	APT1608CGCK

Table 3: A tabulation of all parts used in a PCB

B. Loudspeaker Spec Sheet

SB ACOUSTICS

10” SB29SWNRX-S75-6

Preliminary data

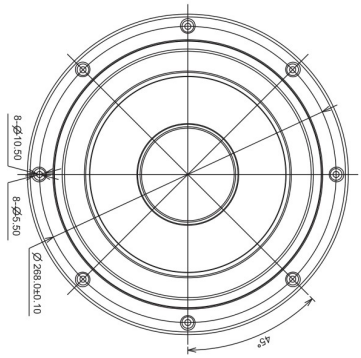

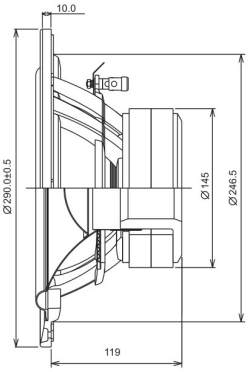

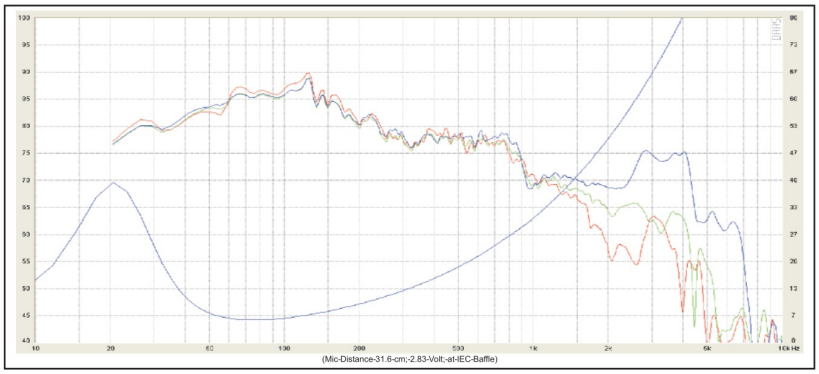

Response-Curve-:

(Blue)-:-on-axis (Green)-:-30-off-axis (-Red-)-: 60-off-axis

Specs :

Nominal-Impedance	6 Ω	Free-air-resonance,-Fs	20-Hz
DC-resistance,-Re	4.5 Ω	Sensitivity-(2.83-V/1m)	86-dB
Voice-coil-inductance,-Le	3.0 mH	Mechanical-Q-factor,-Qms	6.7
Effective-piston-area,-Sd	312 cm^2	Electrical-Q-factor,-Qes	0.33
Voice-coil-diameter	75.6-mm	Total-Q-factor,-Qts	0.31
Voice-coil-height	28.5 mm	Moving-mass-incl.air,-md	132-g
Air-gap-height	6-mm	Force-factor,–Bl	15.1 Tm
Linear-coil-travel-(p-p)	22-mm	Equivalent-volume,-Vas	66-liters
Magnetic-flux-density	0.63 T	Compliance,-Cms	0.48-mm/N
Magnet-weight	2.1-kg	Mechanical-loss,-Rm	2.5-kg/s
Net-weight	5.38 kg	Rated-power-handling	200-watt

The-parameter-are-measured-on-drive-units-that-are-broken-in

Figure 27: Spec Sheet for 10” SB29SWNRX-S75-6 Loudspeaker

C. KiCAD Schematics

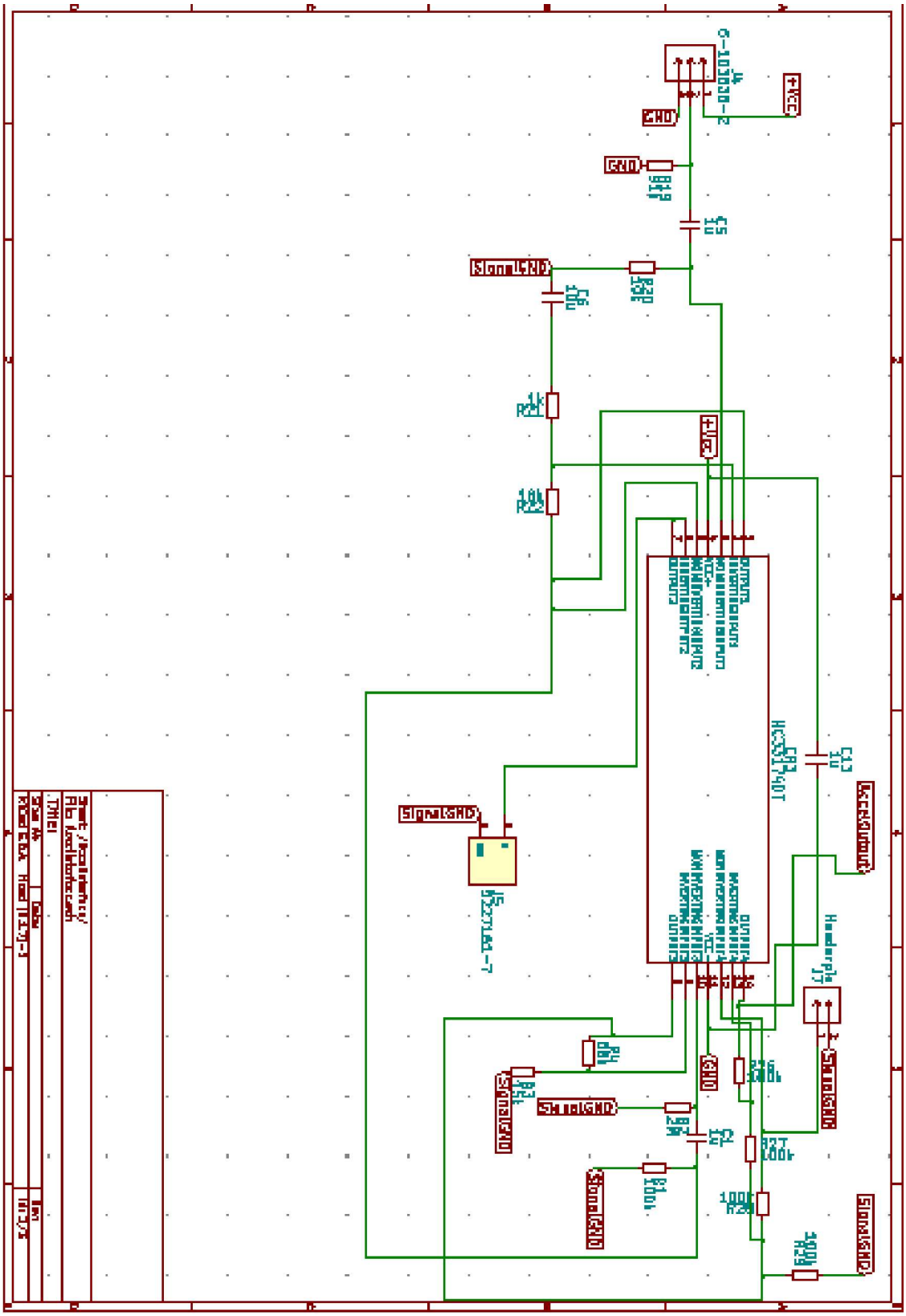

Figure 28: Accelerometer Interface Schematic

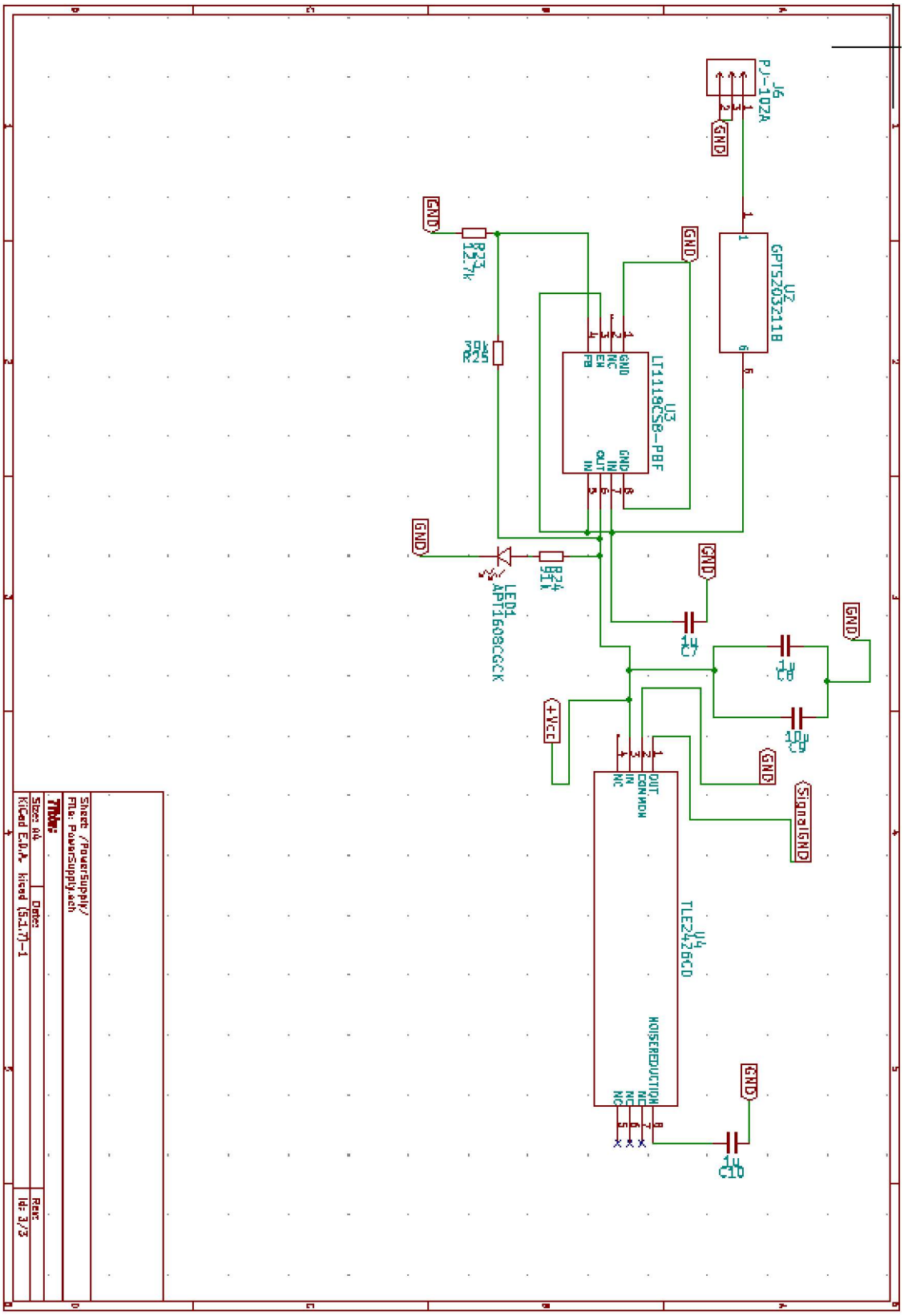

Figure 29: Power Supply Schematic

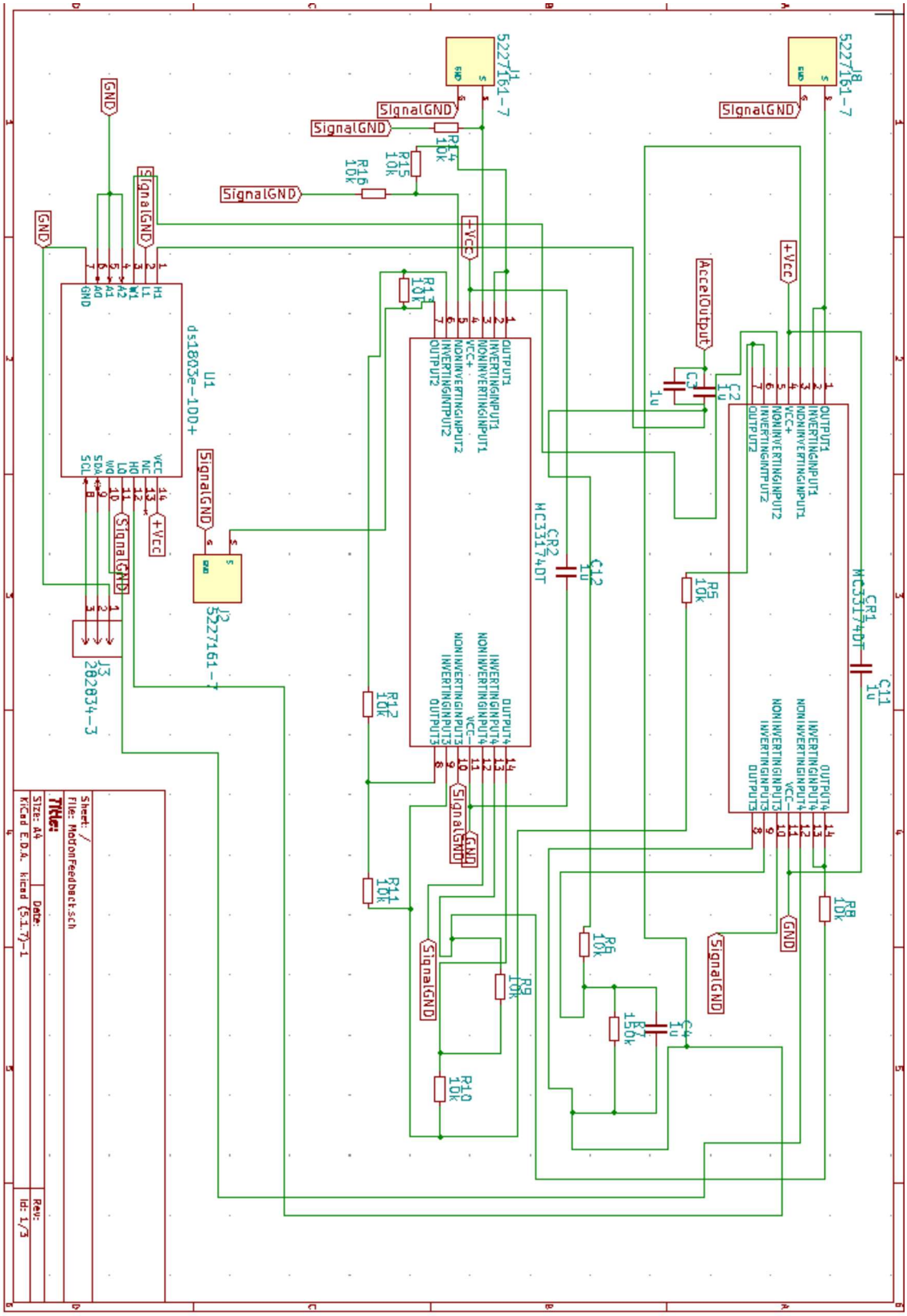

Figure 30: Motional Feedback Schematic

D. Arduino Potentiometer Codes

```
#include <Wire.h>

// To test the Maxim DS1803 dual digital-potentiometer connect:
// VCC, H0, and H1 to 5V on the Arduino
// GND, Ll, L0, A0, A1, and A2 to ground on the Arduino
// SCL and SDA on the DS1803 to SCL and SDA on the Arduino
// If you are not using a MEGA 2560 include pull-up resistors on the SCL and SDA lines
//   See the Wire.h documentation for more information
//
// This code writes independent values to each potentiometer

#include <Wire.h>

void setup()
{
  Wire.begin(); // join i2c bus (address optional for master)
  byte val = 100;
  Wire.beginTransmission(40); // transmit to device 0x28
                              // 0x28 is the address with all 3 pins grounded
  Wire.write(byte(0xAA));     // sends instruction byte,
                              // write to potentiometer-1 (Accel)
  Wire.write(val);            // sends potentiometer value byte
  Wire.endTransmission();     // stop transmitting

   Wire.begin(); // join i2c bus (address optional for master)
  byte val2 = 200;
  Wire.beginTransmission(40); // transmit to device 0x28
  Wire.write(byte(0xA9));     // sends instruction byte,
                              // write to potentiometer-0 (Velo)
  Wire.write(val2);           // sends potentiometer value byte
  Wire.endTransmission();     // stop transmitting
}

void loop() {
  delay(1000);
}
```

Listing 1: Arduino code for independently setting the potentiometer wipers.

E. PCB Board

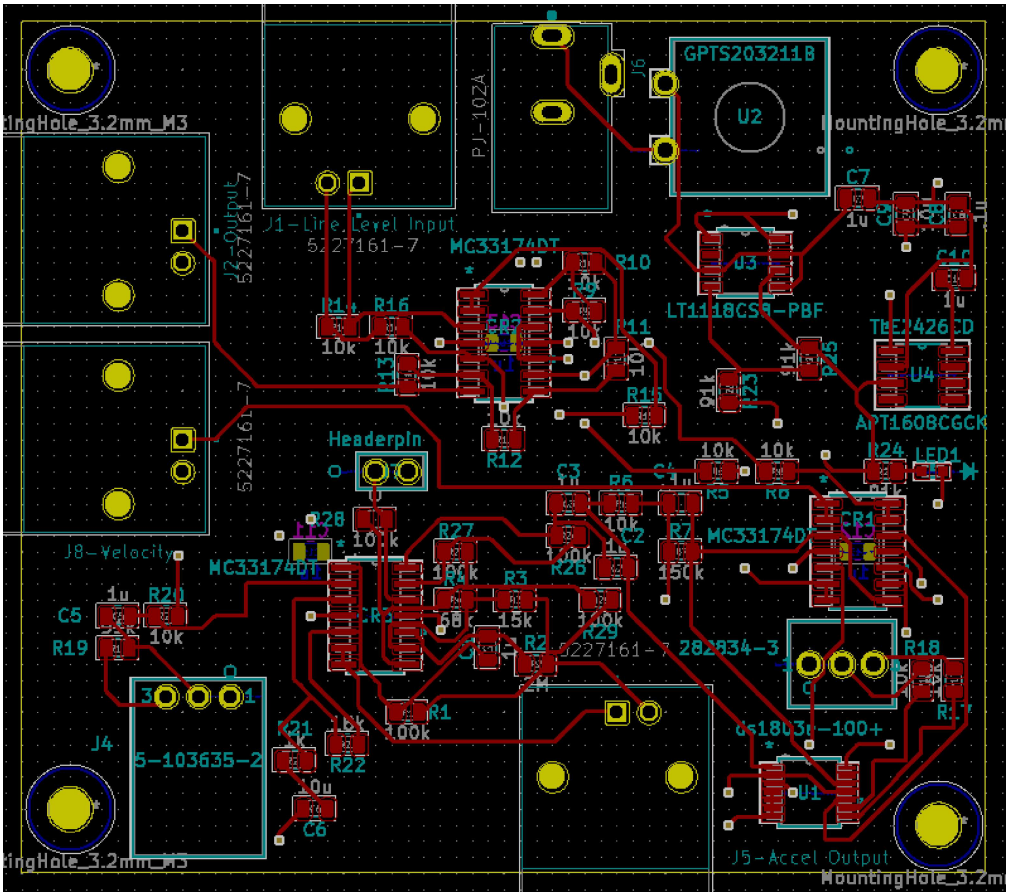

Figure 31: PCB Layout

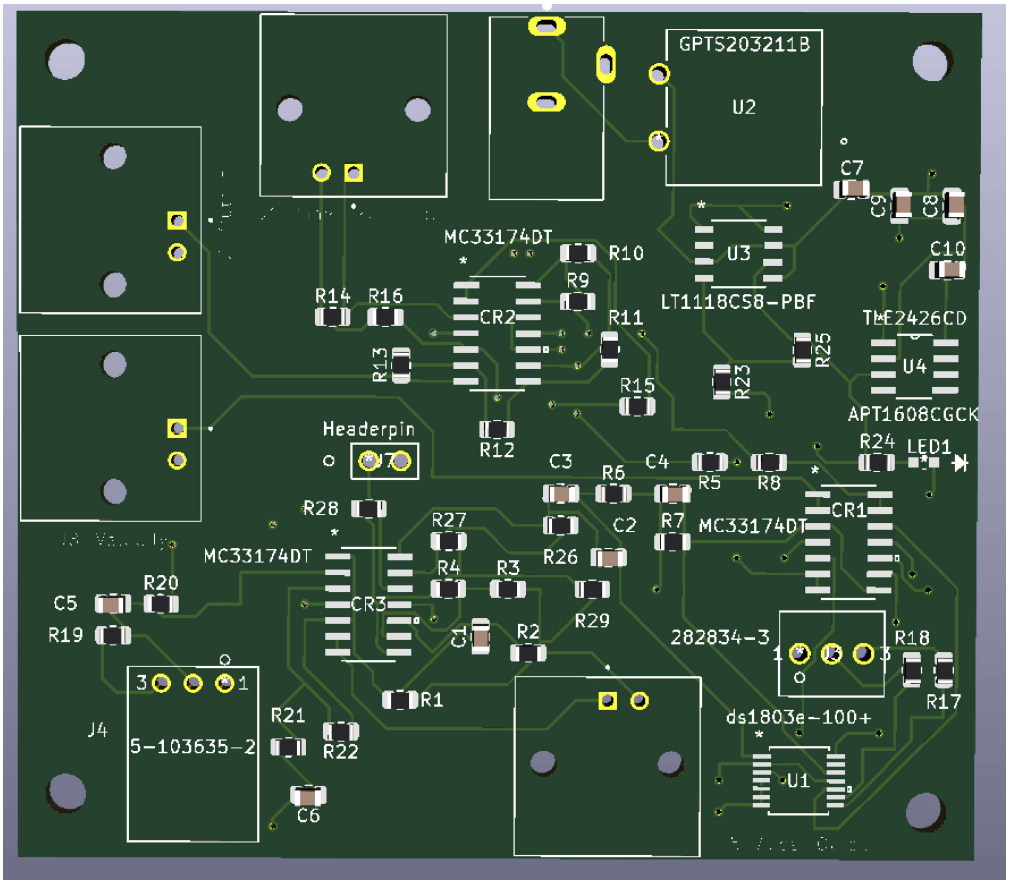

Figure 32: Front Side of 3D Model of PCB Board

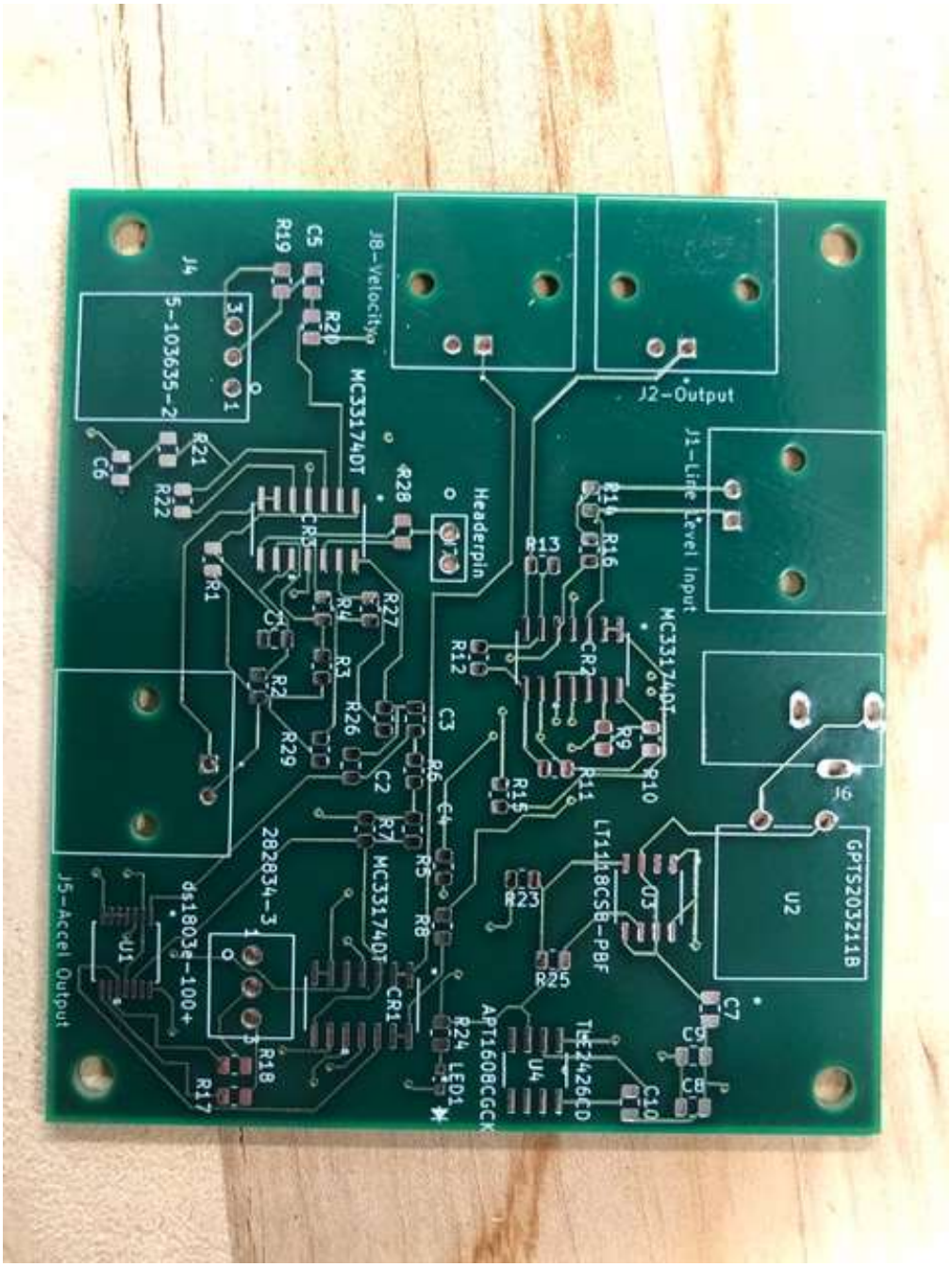

Figure 33: Front Side of PCB Board

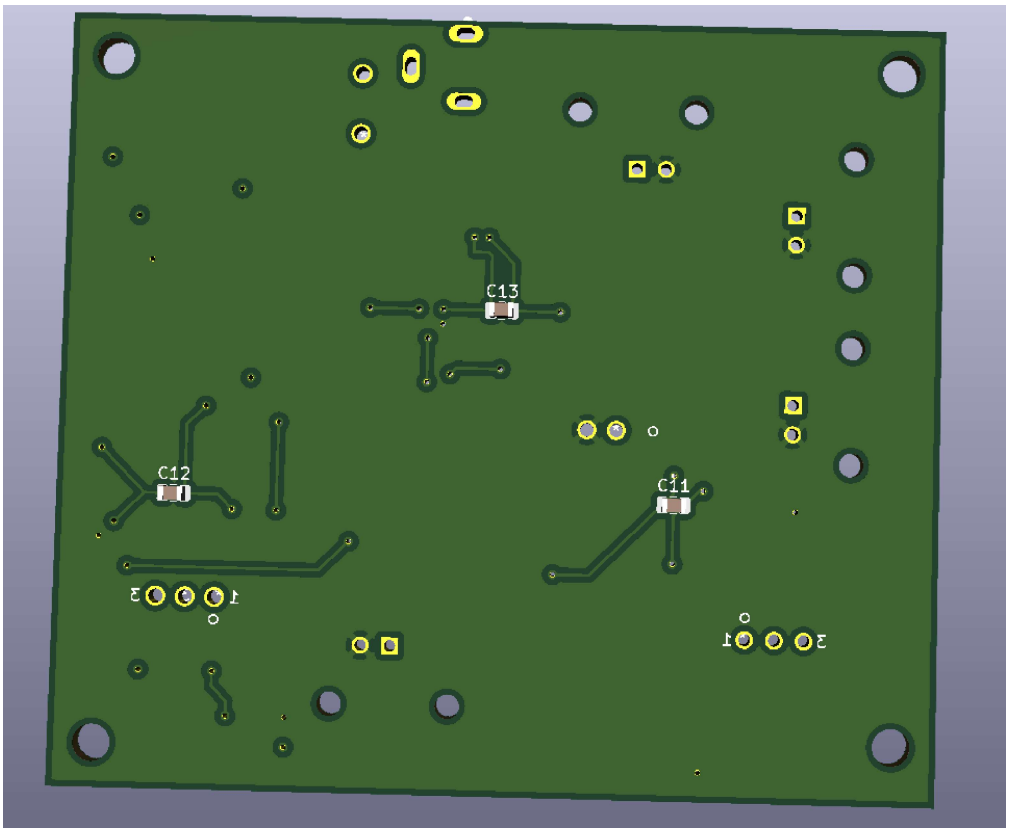

Figure 34: Back Side of 3D Model of PCB Board

F. Accelerometer Plug

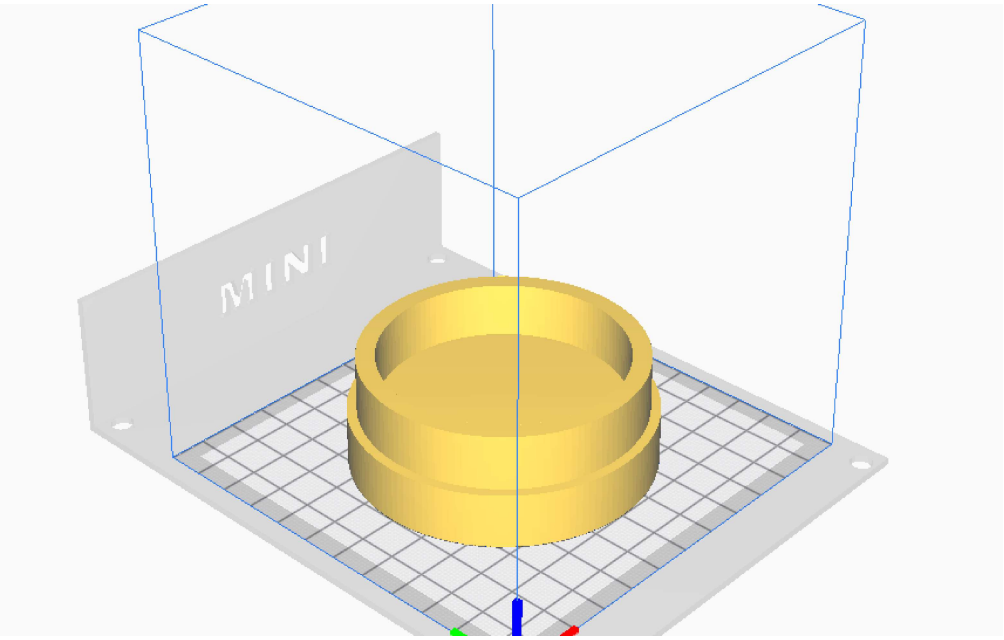

Figure 35: 3D Cura Model for Accelerometer Plug

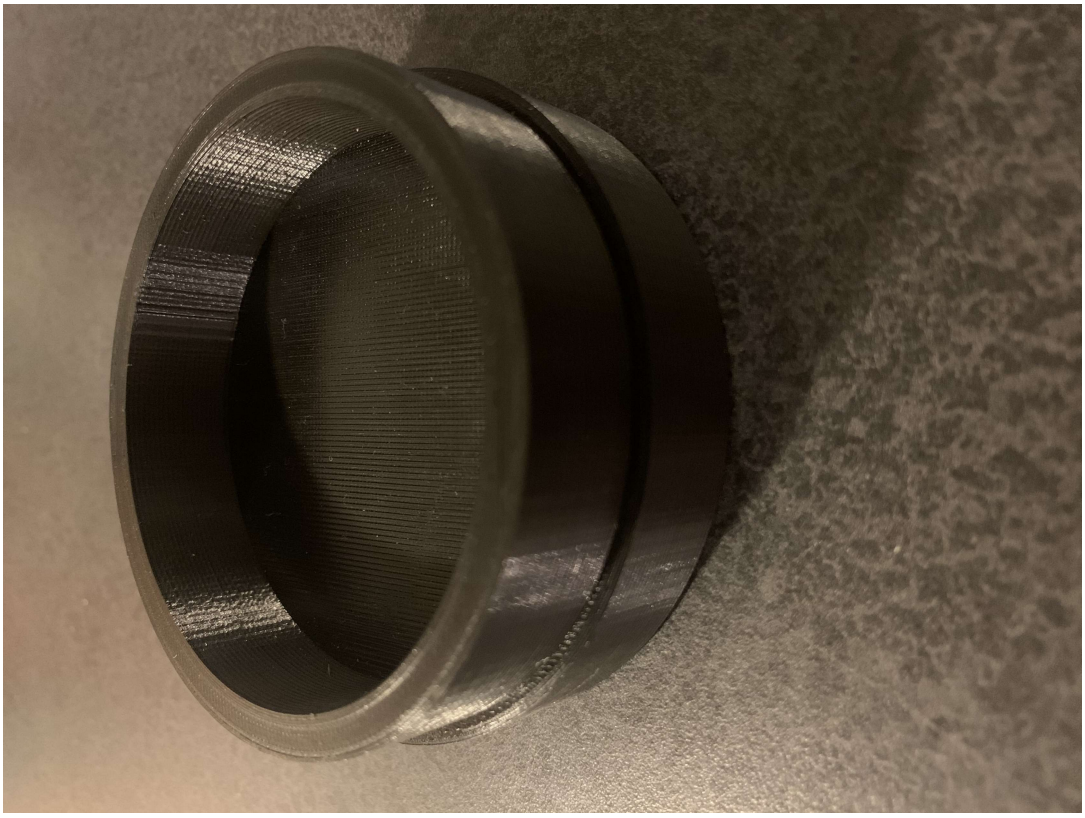

Figure 36: Printed Accelerometer Plug

References

[1] J. W. Marshall Leach, *Introduction to Electroacoustics Audio Amplifier Design*, 4th ed. Kendall Hunt Publishing Company, 2010.

[2] "File:speaker-cross-section.svg," https://commons.wikimedia.org/w/index.php?curid=1530955, accessed: 2021-04-12.

[3] S. Linkwitz, *Linkwitz Lab Sensible Recording and Rendering of Acoustic Scenes*, 2020 (accessed September 29, 2020). [Online]. Available: https://www.linkwitzlab.com/conclusions.htm

[4] R. W. Henderson and P. M. Goggans, "Bayesian comparison of voice coil impedance models for dynaic loudspeakers." AIP, June 2017.

[5] P. Mills and M. Hawksford, "Transconductance power amplifier systems for current-driven loudspeakers," *Journal of the Audio Engineering Society*, vol. 37, no. 10, p. 809, October 1989.